Radiology

# Characterization of Axonal Disease in Patients with Multiple Sclerosis Using High-Gradient-Diffusion MR Imaging[1]

Susie Y. Huang, MD, PhD
Sean M. Tobyne, MA
Aapo Nummenmaa, PhD
Thomas Witzel, PhD
Lawrence L. Wald, PhD
Jennifer A. McNab, PhD
Eric C. Klawiter, MD

**Purpose:** To evaluate the ability of high-gradient-diffusion magnetic resonance (MR) imaging by using gradient strengths of up to 300 mT/m to depict axonal disease in lesions and normal-appearing white matter (NAWM) in patients with multiple sclerosis (MS) and to compare high-gradient-diffusion MR findings in these patients with those in healthy control subjects.

**Materials and Methods:** In this HIPAA-compliant institutional review board–approved prospective study in which all subjects provided written informed consent, six patients with relapsing-remitting MS and six healthy control subjects underwent diffusion-weighted imaging with a range of diffusion weightings performed with a 3-T human MR imager by using gradient strengths of up to 300 mT/m. A model of intra-axonal, extra-axonal, and free water diffusion was fitted to obtain estimates of axon diameter and density. Differences in axon diameter and density between lesions and NAWM in patients with MS were assessed by using the nonparametric Wilcoxon matched-pairs signed rank test, and differences between NAWM in subjects with MS and white matter in healthy control subjects were assessed by using the Mann-Whitney $U$ test.

**Results:** MS lesions showed increased mean axon diameter (10.3 vs 7.9 µm in the genu, 10.4 vs 9.3 µm in the body, and 10.6 vs 8.2 µm in the splenium; $P < .05$) and decreased axon density ([0.48 vs 1.1] $\times 10^{10}/m^2$ in the genu, [0.40 vs 0.70] $\times 10^{10}/m^2$ in the body, and [0.35 vs 1.1] $\times 10^{10}/m^2$ in the splenium; $P < .05$) compared with adjacent NAWM. No significant difference in mean axon diameter or axon density was detected between NAWM in subjects with MS and white matter in healthy control subjects.

**Conclusion:** High-gradient-diffusion MR imaging using gradient strengths of up to 300 mT/m can be used to characterize axonal disease in patients with MS, with results that agree with known trends from neuropathologic data showing increased axon diameter and decreased axon density in MS lesions when compared with NAWM.

©RSNA, 2016

*Online supplemental material is available for this article.*

The detection of clinically relevant changes in axonal microstructure is essential to understanding the mechanisms of disease progression in patients with multiple sclerosis (MS) and improving patient care. Conventional MR imaging has high sensitivity in the detection of demyelination of lesions but falls short in the characterization of axonal damage that is thought to be the substrate for clinical disability (1,2). Even advanced magnetic resonance (MR) techniques, such as diffusion-tensor imaging, have not shown robust pathologic specificity for axonal damage (3–7). The need for imaging biomarkers specific to axonal damage in patients with MS motivates the development of new techniques that are sensitive to the underlying white matter microstructure.

Diffusion MR imaging sensitizes the MR signal to the Brownian motion of water and provides insight into the microenvironment of different tissue types and structures at the micron scale, which is below the spatial resolution of the MR image. Several diffusion MR techniques with which to quantify axon diameter and packing density in white matter have emerged relatively recently (8–10). The sensitivity of these techniques to small-diameter axons is limited by the maximum gradient strength of clinical MR imagers (11,12). In vivo attempts to apply these methods at a clinical gradient strength of 40–60 mT/m (10) have yielded limited diffusion resolution and have led to overestimation of axonal size when compared with known values from histologic analysis (13). The relatively recent availability of higher maximum gradient strengths on human MR imagers (14,15), including a 3-T human MR imager equipped with 300 mT/m gradients (14), has enabled the translation of these methods from animal (9) and ex vivo (8,10) studies to the in vivo human brain (10,12,16). We have shown that use of maximum gradient strengths up to 300 mT/m decreases mean axon diameter estimates in vivo by at least two to three times when compared with conventional gradient strengths and also decreases uncertainty in the estimates (12). Such technologic advancements offer unprecedented resolution of micron-sized axons (12,16) in the living human brain.

We hypothesized that MS lesions on high-gradient-diffusion MR images obtained by using a gradient strength of up to 300 mT/m would show decreased axon density and increased axon diameter, as has been shown in prior histopathologic studies (17–19). The purpose of this study was to evaluate the ability of high-gradient-diffusion MR imaging using gradient strengths of up to 300 mT/m to characterize axonal disease in lesions and normal-appearing white matter (NAWM) in patients with MS and to compare high-gradient-diffusion MR findings in these patients with those in healthy control subjects.

## Materials and Methods

This prospective study was approved by the institutional review board and was compliant with Health Insurance Portability and Accountability Act guidelines. All participants provided written informed consent.

### Study Participants

Six patients with relapsing-remitting MS and six age- and sex-matched healthy volunteers were prospectively recruited from August 2012 through March 2014. Inclusion criteria for MS subjects were age of 18–60 years, fulfillment of 2010 revised McDonald criteria for relapsing-remitting MS (20), Expanded Disability Status Scale score of 2.0–6.5, and one corpus callosum lesion on clinical fluid-attenuated inversion recovery (FLAIR) images. Exclusion criteria were clinical relapse within the past 3 months, evidence of other structural brain disease, and severe claustrophobia or another

### Advances in Knowledge

- High-gradient-diffusion MR imaging using gradient strengths of up to 300 mT/m is a method that can be used to perform in vivo quantification of axon diameter and axon density, with unprecedented diffusion resolution in lesions and normal-appearing white matter in patients with multiple sclerosis (MS).

- High-gradient-diffusion MR measurements of axon diameter and axon density using gradient strengths of up to 300 mT/m show significantly increased mean axon diameter (10.3 vs 7.9 $\mu$m in the genu, 10.4 vs 9.3 $\mu$m in the body, and 10.6 vs 8.2 $\mu$m in the splenium; $P < .05$) and decreased axon density ([0.48 vs 1.1] $\times 10^{10}/m^2$ in the genu, [0.40 vs 0.70] $\times 10^{10}/m^2$ in the body, and [0.35 vs 1.1] $\times 10^{10}/m^2$ in the splenium; $P < .05$) in MS lesions compared with those in adjacent normal-appearing white matter.

### Implication for Patient Care

- High-gradient-diffusion MR imaging with a gradient strength of up to 300 mT/m offers a noninvasive tool with which to study axonal disease in patients with MS.

### Table 1

**Characteristics and Clinical Status of Healthy Control Subjects and Relapsing-Remitting Patients with MS**

| Characteristic and Clinical Status | Healthy Control Subjects | Relapsing-Remitting Patients with MS |
|---|---|---|
| No. of subjects | 6 | 6 |
| Sex ratio (male-to-female) | 4:2 | 3:3 |
| Age (y)* | 30.7 ± 9.0 | 34.2 ± 8.2 |
| Disease duration (y)* | NA | 6.4 ± 4.7 |
| Median EDSS | NA | 1.5 (1.0–3.0)† |

Note.—EDSS = Expanded Disability Status Scale, NA = not applicable.

* Data are mean ± standard deviation.

† Data in parentheses are the range.

contraindication to MR imaging. All participants enrolled in this study met all inclusion criteria. No patients or control subjects were excluded. Demographic and clinical characteristics of patients with MS and healthy control subjects are summarized in Table 1.

### Imaging Technique

All subjects were examined with a dedicated high-gradient (AS302) 3-T MR imager (Magnetom Connectom; Siemens Healthcare, Erlangen, Germany) with a maximum gradient strength of 300 mT/m and a maximum slew rate of 200 T/m/sec. A custom-made 64-channel phased-array head coil was used for signal reception (14). Sagittal 2-mm isotropic resolution diffusion-weighted stimulated echo echo-planar images were acquired with 17 contiguous sections in the midline corpus callosum. We chose a voxel size of 2 mm to achieve sufficient signal-to-noise ratio while minimizing partial volume effects near the ventricles and thin portions of the corpus callosum. The following imaging parameters were used: repetition time msec/echo time msec, 3100/54; gradient pulse duration δ, 8.7 msec; 17 diffusion gradient increments (25–241 mT/m); and 12 signal averages acquired. The experiment was repeated for five diffusion times: 35, 44, 54, 84, and 120 msec. Diffusion gradients were applied in the $z$ direction orthogonal to the fibers in the corpus callosum. Interspersed T2-weighted ($b$ = 0 sec/mm²)

images were acquired for each diffusion gradient–time combination. The maximum $b$ value at the longest diffusion time was 10 000 sec/mm². Representative diffusion-weighted images are shown in Figure E1 (online). The total diffusion examination time was 53 minutes.

FLAIR images were acquired to assist in lesion localization by using the following parameters: repetition time msec/echo time msec/inversion time msec, 5000/389/1800; 0.4 × 0.4 × 0.9 mm voxels; 192 sagittal sections; in-plane image matrix, 256 × 256;, and parallel imaging using generalized autocalibrating partially parallel acquisitions with an acceleration factor of two. The FLAIR sequence lasted 6 minutes.

The data preprocessing pipeline, including gradient nonlinearity, eddy current, and motion correction, have been described in detail previously (12,16). In brief, to correct for interexamination bulk motion during the diffusion sequence, the interspersed T2-weighted images ($b$ = 0 sec/mm²) acquired with each diffusion gradient and time combination were used to coregister all images with FLIRT software *(www.fmrib.ox.ac.uk/fsl)*. Physiologic motion due to cardiac pulsation was not substantial in the corpus callosum based on inspection of the raw diffusion data. Image warping caused by gradient nonlinearity was corrected by calculating the three-dimensional displacements generated by nonlinear terms in the

magnetic field for each gradient coil (21). Correction of eddy current–induced distortions was achieved by using opposite-polarity diffusion-weighted imaging pairs (22), which were registered one to the other, constraining for expected translations and dilations in the phase-encoding direction and for shears in the section plane. The halfway transform was then calculated and applied to each diffusion-weighted image. To facilitate mapping of lesions on diffusion-weighted images in patients with MS, the FLAIR images were coregistered to the T2-weighted images ($b$ = 0 sec/mm²) with the aforementioned software.

### Data Analysis

Diffusion in the corpus callosum was modeled as occurring in three compartments: restricted intra-axonal diffusion, hindered extra-axonal diffusion, and free diffusion in cerebrospinal fluid. The model was then fitted to the data to obtain maps of the following parameters: axon diameter, restricted fraction, and free water fraction. A detailed description of the signal model and model fitting is provided in Appendix E1 (online).

Two experienced readers (S.Y.H., S.M.T.; 12 years of experience combined) drew regions of interest (ROIs) of nine voxels each in the midline sagittal corpus callosum within NAWM of the genu, body, and splenium in subjects with MS and in similar locations in healthy control subjects. MS lesion ROIs were drawn on midline sagittal FLAIR images, excluding edge voxels abutting the ventricles. The number of voxels for the lesion ROIs ranged from two to five, given variable lesion size in different subjects. The mean of the posterior distribution for each parameter was calculated on a voxelwise basis using a Rician noise model, as described in Appendix E1 (online). The estimated posterior means were then combined for voxels within each ROI to derive summary statistics (ie, mean and standard deviation across the ROI) of the fitted parameters. Axon density was calculated by weighting the restricted fraction by the cross-sectional area based on mean axon diameter.

## Statistical Analysis

Mean axon diameter, restricted fraction, cerebrospinal fluid fraction, and axon density were compared between MS lesion ROIs and NAWM ROIs in the same patients with MS by using the nonparametric Wilcoxon matched-pairs signed rank test and between NAWM in patients with MS and white matter in healthy control subjects by using the Mann-Whitney $U$ test. All statistical analyses were performed by using Statistical Package for the Social Sciences, version 21 (SPSS, Chicago, Ill).

## Results

Figure 1 shows estimates of axon diameter, restricted fraction, free water fraction, and axon density for each healthy control subject and patient with MS. Table 2 presents group mean estimates of axon diameter, restricted fraction, free water fraction, and axon density in the genu, body, and splenium in all healthy control subjects and for corresponding NAWM and lesions in all patients with MS. On a group level, MS lesions showed significantly larger mean axon diameter (Fig 1, B) compared with adjacent NAWM (10.3 vs 7.9 μm in the genu, 10.4 vs 9.2 μm in the body, and 10.6 vs 8.2 μm in the splenium; $P$ = .028). MS lesions also had significantly decreased mean restricted fraction (Fig 1, D) compared with NAWM (0.39 vs 0.53 in the genu, 0.30 vs 0.45 in the body, and 0.27 vs 0.55 in the splenium; $P$ = .028). Mean free water fraction was significantly higher in MS lesions (Fig 1, F) than in NAWM (0.02 vs 0.01 in the genu, 0.03 vs 0.01 in the body, and 0.02 vs 0.01 in the splenium; $P$ = .028). Mean axon density was significantly reduced in MS lesions (Fig 1, H) compared with NAWM ([0.48 vs 1.1] $\times$ $10^{10}$/ $m^2$ in the genu, [0.40 vs 0.70] $\times$ $10^{10}$/ $m^2$ in the body, and [0.35 vs 1.1] $\times$ $10^{10}$/$m^2$ in the splenium; $P$ = .028). No significant difference in mean axon diameter, restricted fraction, free water fraction, or axon density was seen between NAWM in patients with MS and similar locations in healthy control subjects.
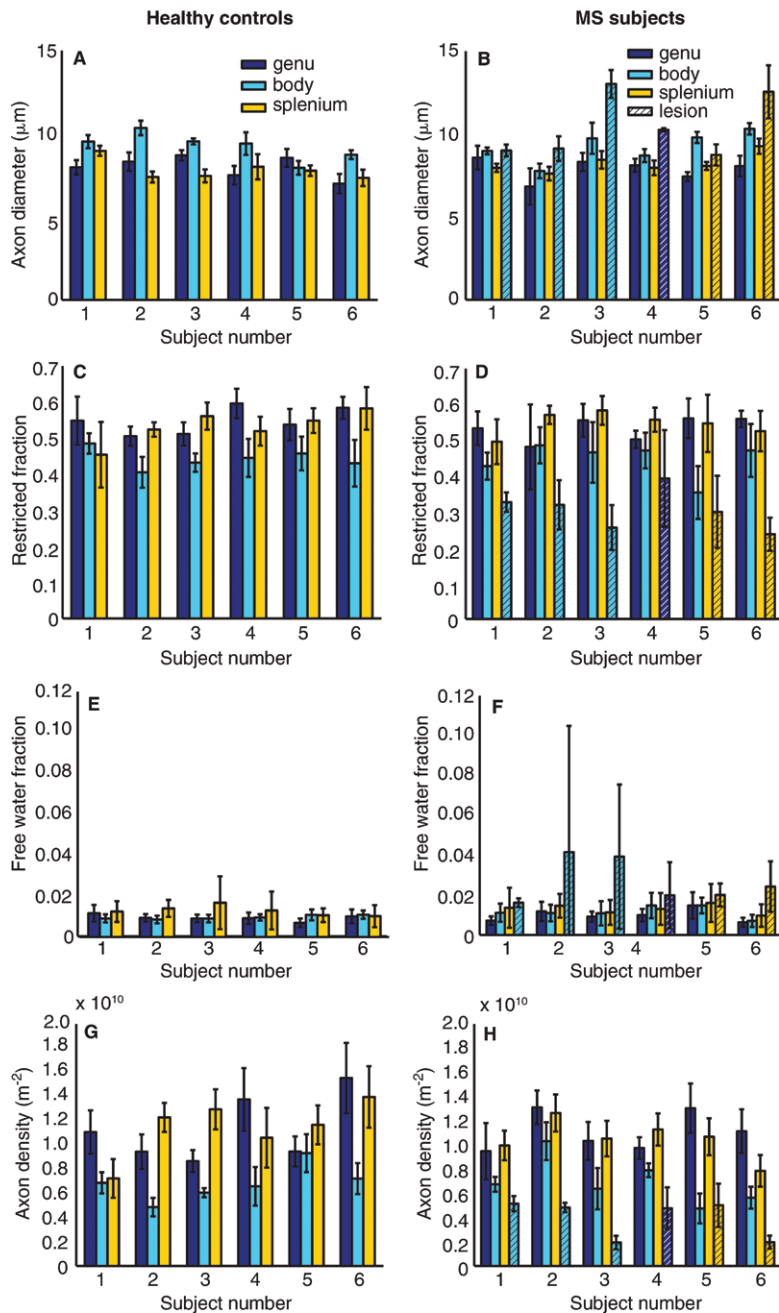


**Figure 1:** Mean $\pm$ standard deviation of estimates for, *A, B*, axon diameter; *C, D*, restricted fraction; *E, F*, free water fraction; and, *G, H*, axon density in the six healthy control subjects and six patients with MS within ROIs drawn in NAWM in the genu, body, and splenium of the midline sagittal section of the corpus callosum in the patients with MS and in similar locations in the healthy control subjects. The estimates for axon diameter *(B)*, restricted fraction *(D)*, free water fraction *(F)*, and axon density *(H)* within the lesion for each patient with MS are indicated as bars with hatch marks and are color coded to match the location of the corresponding normal-appearing areas of the corpus callosum.

Radiology

**Table 2**

**Estimates of Axon Diameter, Restricted Fraction, Free Water Fraction, and Axon Density in Healthy Control Subjects and NAWM and Lesions in Patients with MS**

| Measurement | Healthy Control Subjects | | | NAWM in Patients with MS | | | Lesions in Patients with MS | | |
|---|---|---|---|---|---|---|---|---|---|
| | Genu | Body | Splenium | Genu | Body | Splenium | Genu* | Body | Splenium |
| Axon diameter (μm) | 8.00 ± 0.66 | 9.25 ± 0.82 | 7.82 ± 0.62 | 7.89 ± 0.64 | 9.22 ± 0.92 | 8.22 ± 0.58 | 10.3 | 10.4 ± 0.23 | 10.6 ± 0.27 |
| Restricted fraction | 0.55 ± 0.04 | 0.44 ± 0.03 | 0.53 ± 0.04 | 0.53 ± 0.03 | 0.45 ± 0.05 | 0.55 ± 0.03 | 0.39 | 0.30 ± 0.04 | 0.27 ± 0.04 |
| Free water fraction | 0.01 ± 0.002 | 0.01 ± 0.001 | 0.01 ± 0.002 | 0.01 ± 0.003 | 0.01 ± 0.003 | 0.01 ± 0.002 | 0.02 | 0.03 ± 0.01 | 0.02 ± 0.003 |
| Axon density (× $10^{10}$/m²) | 1.13 ± 0.27 | 0.68 ± 0.15 | 1.14 ± 0.24 | 1.11 ± 0.16 | 0.70 ± 0.20 | 1.05 ± 0.16 | 0.48 | 0.40 ± 0.18 | 0.35 ± 0.22 |

Note.—Data are mean ± standard deviation.
* Standard deviations were not calculated, as only one patient had a lesion in the genu.

Figure 2 shows voxelwise estimates of mean axon diameter, restricted fraction, and axon density for the midline sagittal corpus callosum of each patient with MS. Lesions showed larger axon diameters and reduced restricted fraction and axon density when compared with those of adjacent NAWM. Regional variations in axon diameter and density were also evident, with smaller diameter and more tightly packed axons in the genu and splenium when compared with those in the body.

Figure 3 compares the measured signal with predictions from model fitting to the ROI-averaged signal from representative voxels in the genu, body, and splenium NAWM, as well as in a selected lesion in the body of the corpus callosum in a patient with MS (patient 3). Mere visual inspection of the signal decay curves in Figure 3 reveals differences between different regions of the corpus callosum and between lesions and NAWM, which is reflected in the differences in fitted axon diameter and density between lesions and NAWM and suggests differences in the underlying microstructure. The signal-to-noise ratio of the data was approximately 20. The model was considered to be an adequate representation of the data based on comparison of the predicted signal and the diffusion-weighted data points shown in Figure 3. The residuals, represented as the difference between the predicted and measured signal in each region of the corpus callosum, followed a Gaussian distribution with a standard deviation of approximately 0.05, which corresponded to a signal-to-noise ratio of 20. Given that the magnitude and distribution of the residuals matched those of the expected noise level, the data fit using the model described in this article was considered adequate.

## Discussion

This pilot study shows the feasibility of using high-gradient-diffusion MR imaging with gradient strengths up to 300 mT/m for in vivo characterization of axonal disease in patients with MS. MS lesions showed significantly larger axon diameters and decreased axon density when compared with corresponding NAWM. Possible mechanisms for larger axon diameters in MS lesions include selective loss of smaller-diameter axons or an increase in diameter of preserved axons for faster impulse conduction in the presence of demyelination and axonal loss.

The findings presented in this study are in agreement with reported histopathologic observations of larger axon diameter and decreased axon density in MS lesions as compared with NAWM (17–19). In our study, no significant difference in axon diameter, free water fraction, or axon density was noted in NAWM in patients with MS or in healthy control subjects. Previous histologic studies in the spinal cord of patients with MS have shown a marked decrease in axon density and larger axonal diameter in both lesions and NAWM when compared with those in healthy control subjects (17,18). The few studies that reported axon diameter and density in pathologic specimens involved tissues of chronic lesions in patients with long-standing progressive MS that were studied at autopsy (17–19). Changes in axon diameter and density in NAWM may be more readily appreciated in patients with longer disease duration and more severe disability. To improve the sensitivity of axon diameter estimates to axonal pathology in NAWM in patients with MS, it may be helpful to study patients with a more advanced stage of the disease, in whom widespread axonal degeneration would be expected.

By modeling water diffusion in the intra- and extra-axonal compartments, our approach and other microstructural methods based on *q*-space imaging, such as AxCaliber (8) and ActiveAx (10), offer the ability to quantify the relative contributions of intra- and extra-axonal diffusion, which may provide improved pathologic specificity for axonal loss compared with more commonly used diffusion-tensor imaging metrics (5). Other recent approaches, such as diffusion basis spectrum imaging (or DBSI) also include an isotropic diffusion component in modeling white matter diffusion to account for
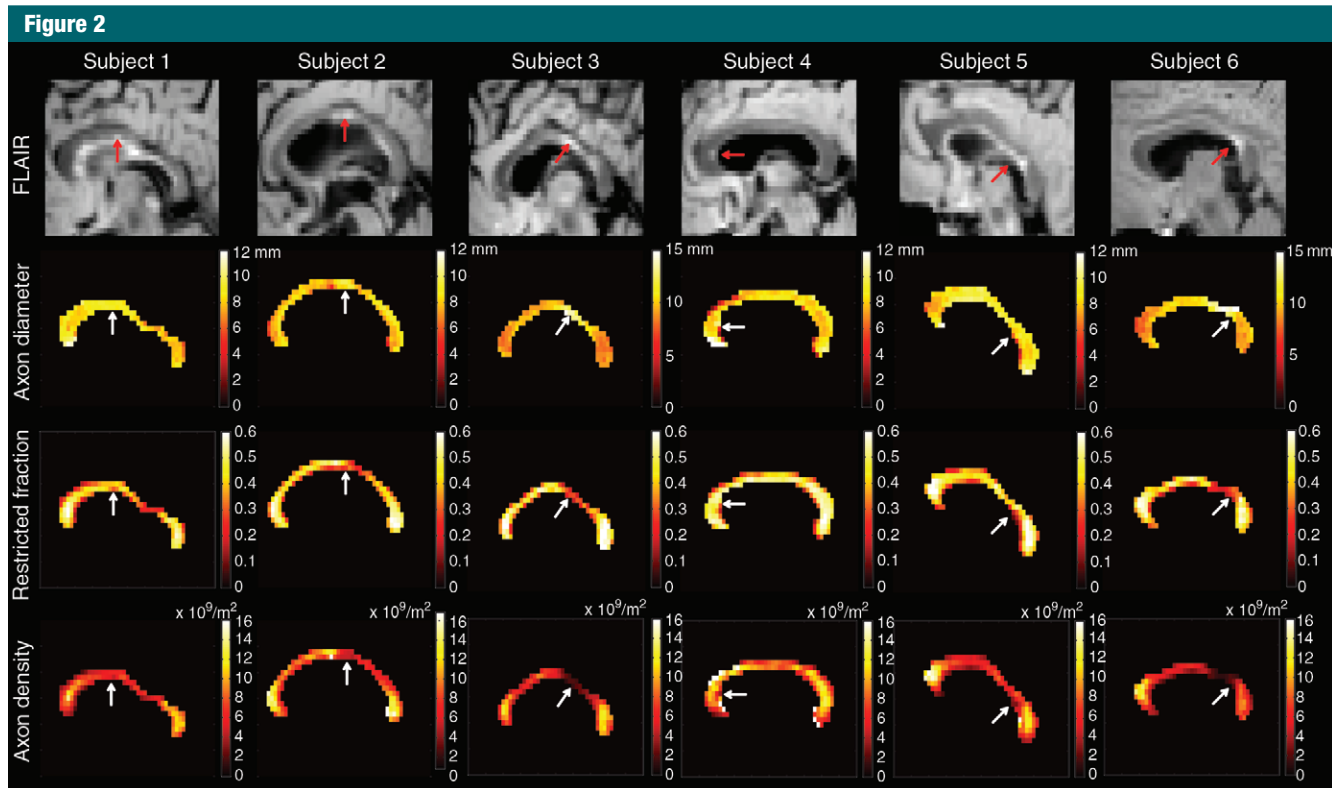
Radiology

**Figure 2**



**Figure 2:** Sagittal FLAIR images (top row) and voxelwise maps of axon diameter (second row), restricted fraction (third row), and axon density (bottom row) in the midline corpus callosum in the six patients with MS. Lesions can be seen on FLAIR images (red arrows) and voxelwise maps (white arrows). Lesions show increased axon diameter and decreased restricted fraction and axon density, as compared with the adjacent NAWM.

increased edema in MS lesions (23). The improved specificity of axial diffusivity, radial diffusivity, and restricted diffusion tensor fraction obtained with diffusion basis spectrum imaging may reflect axonal injury, myelin integrity, and inflammation-associated cellularity change (24). Similarly, our estimates of axon diameter and density within lesions may provide better pathologic specificity by accounting for increased free water associated with lesions.

This study had a number of limitations. The small sample size made it difficult to generalize the findings; however, even this small group of patients showed significant differences in axon diameter and density in MS lesions when compared with NAWM. This finding was in agreement with previously reported trends seen at histopathologic analysis. The correlation of axon diameter and density with clinical disability would elucidate the

relationship of axonal degeneration to clinical disability in patients with MS and the effects of current and future MS therapies on axonal integrity, which are currently unknown. The small sample size prevented us from doing any robust clinical correlation with Expanded Disability Status Scale scores; however, future studies aimed at expanding the sample size will be specifically designed to answer this question. In addition, the estimated axon diameters were larger (approximately 8–10 μm) than expected (<5 μm), leading us to conclude that the estimated axon diameter may not be a fully quantitative measurement. Potential confounding factors included the use of long diffusion times (12) and failure to account for orientation dispersion (25). Rather than serving as fully quantitative measures of mean axon diameter and density, our measurements may be considered as axon

diameter and density-weighted images that capture broad trends in axon size. Another limitation of the current work is the long time needed for the diffusion acquisition. Our acquisition was designed to be comprehensive to ensure that there would be sufficient data and signal-to-noise ratio for model fitting. Current efforts are focused on optimizing the examination to minimize the number of diffusion times and gradient strengths needed for model fitting, such that the sequence will fit within a clinically feasible examination time. Finally, the validity of using the same model for healthy white matter and axonal disease remains an open question. The free water fraction accounted for the expected increase in extracellular space within MS lesions secondary to gliosis and axonal loss. Our model provided a reasonable fit to the data in NAWM and lesions in a representative patient with MS and
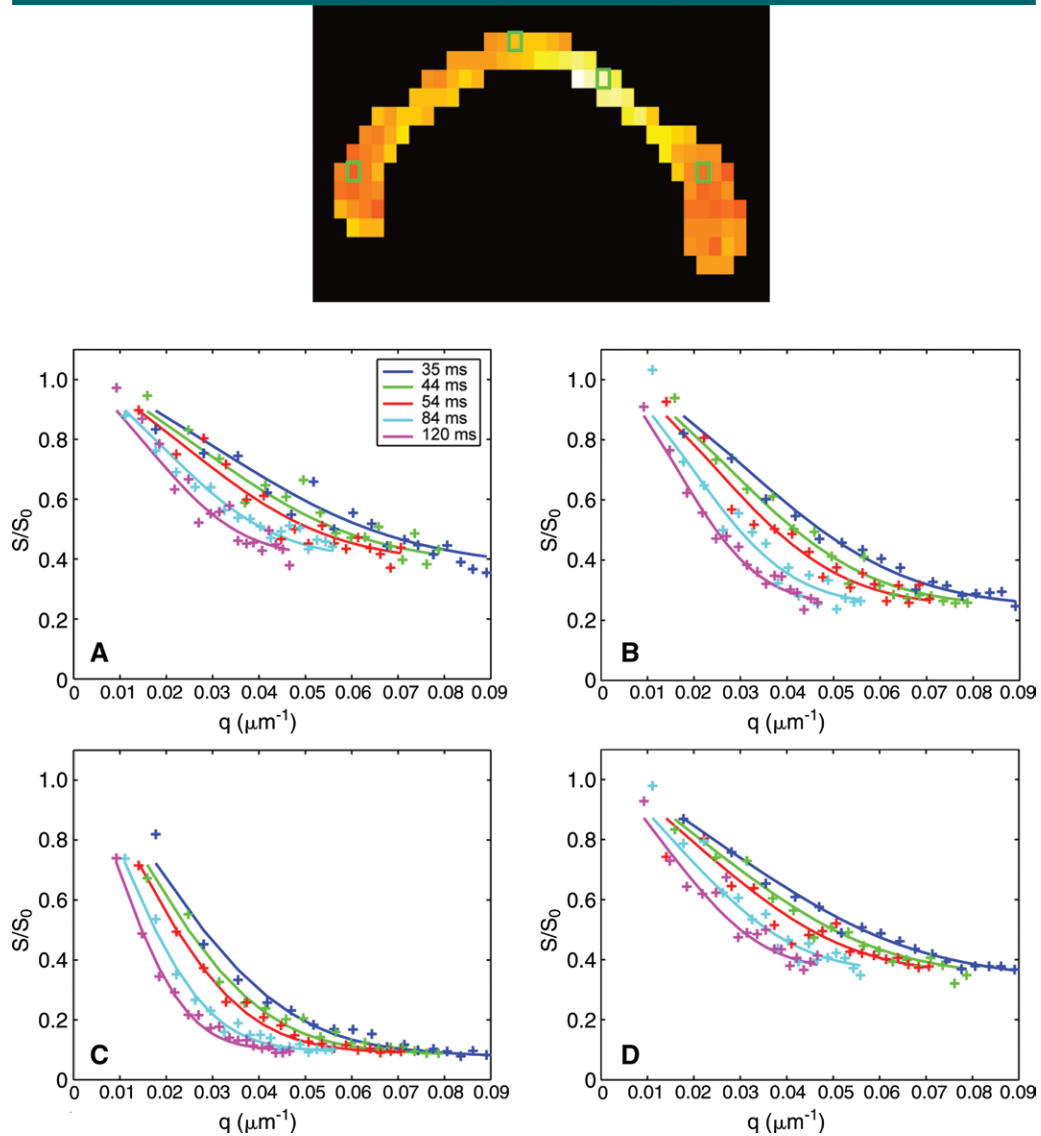
**Figure 3:** Sagittal axon diameter map (top image) shows representative voxels in the, *A*, genu; *B*, body; *C*, lesion; and, *D*, splenium of the midline corpus callosum in a patient with MS (patient 3) and corresponding diffusion-weighted data and fitted signal decays for different *q* and diffusion times. The solid lines represent the predicted signals from the fitted model. All measurements were normalized by an estimate of $S_0$, the signal obtained without diffusion weighting ($b = 0$).

showed similar errors in the estimates for NAWM and MS lesions, which lends support to the current model.

High-gradient-diffusion MR imaging with gradient strengths of up to 300 mT/m is feasible in the characterization of axonal disease in patients with MS and yields axon diameter and density estimates in lesions and NAWM that agree with known trends from histopathologic data. The use of high gradient strengths of up to 300 mT/m in the accurate in vivo characterization of white matter microstructure motivates the development of stronger gradients for clinical MR imagers and will in turn inform our understanding of how axon diameter estimates change at lower gradient strengths. By providing specific measures of axon diameter and density in vivo, we offer a noninvasive imaging biomarker for axonal damage, the hypothesized substrate for clinical disability in patients with MS. Further studies are needed to correlate axon diameter and density measurements with direct histopathologic characterization of axonal damage in patients with MS, as well as to evaluate the relationship of these metrics with clinical disability.

### References

1. Dutta R, Trapp BD. Mechanisms of neuronal dysfunction and degeneration in multiple sclerosis. Prog Neurobiol 2011;93(1):1–12.

2. Barkhof F. The clinico-radiological paradox in multiple sclerosis revisited. Curr Opin Neurol 2002;15(3):239–245.

3. Schmierer K, Wheeler-Kingshott CA, Boulby PA, et al. Diffusion tensor imaging of post mortem multiple sclerosis brain. Neuroimage 2007;35(2):467–477.

4. Roosendaal SD, Geurts JJ, Vrenken H, et al. Regional DTI differences in multiple sclerosis patients. Neuroimage 2009;44(4):1397–1403.

5. Klawiter EC, Schmidt RE, Trinkaus K, et al. Radial diffusivity predicts demyelination in ex vivo multiple sclerosis spinal cords. Neuroimage 2011;55(4):1454–1460.

6. Sbardella E, Tona F, Petsas N, Pantano P. DTI measurements in multiple sclerosis: evaluation of brain damage and clinical implications. Mult Scler Int 2013;2013:671730.

7. Lee JY, Taghian K, Petratos S. Axonal degeneration in multiple sclerosis: can we predict and prevent permanent disability? Acta Neuropathol Commun 2014;2:97.

8. Assaf Y, Blumenfeld-Katzir T, Yovel Y, Basser PJ. AxCaliber: a method for measuring axon diameter distribution from diffusion MRI. Magn Reson Med 2008;59(6):1347–1354.

9. Barazany D, Basser PJ, Assaf Y. In vivo measurement of axon diameter distribution in the corpus callosum of rat brain. Brain 2009;132(Pt 5):1210–1220.

10. Alexander DC, Hubbard PL, Hall MG, et al. Orientationally invariant indices of axon diameter and density from diffusion MRI. Neuroimage 2010;52(4):1374–1389.

11. Dyrby TB, Sogaard LV, Hall MG, Ptito M, Alexander DC. Contrast and stability of the axon diameter index from microstructure imaging with diffusion MRI. Magn Reson Med 2013;70(3):711–721.

12. Huang SY, Nummenmaa A, Witzel T, et al. The impact of gradient strength on in vivo diffusion MRI estimates of axon diameter. Neuroimage 2015;106:464–472.

13. Aboitiz F, Scheibel AB, Fisher RS, Zaidel E. Fiber composition of the human corpus callosum. Brain Res 1992;598(1-2):143–153.

14. Setsompop K, Kimmlingen R, Eberlein E, et al. Pushing the limits of in vivo diffusion MRI for the Human Connectome Project. Neuroimage 2013;80:220–233.

15. Van Essen DC, Ugurbil K, Auerbach E, et al. The Human Connectome Project: a data acquisition perspective. Neuroimage 2012;62(4):2222–2231.

16. McNab JA, Edlow BL, Witzel T, et al. The Human Connectome Project and beyond: initial applications of 300 mT/m gradients. Neuroimage 2013;80:234–245.

17. Lovas G, Szilágyi N, Majtényi K, Palkovits M, Komoly S. Axonal changes in chronic demyelinated cervical spinal cord plaques. Brain 2000;123(Pt 2):308–317.

18. Bergers E, Bot JC, De Groot CJ, et al. Axonal damage in the spinal cord of MS patients occurs largely independent of T2 MRI lesions. Neurology 2002;59(11):1766–1771.

19. Fisher E, Chang A, Fox RJ, et al. Imaging correlates of axonal swelling in chronic multiple sclerosis brains. Ann Neurol 2007;62(3):219–228.

20. Polman CH, Reingold SC, Banwell B, et al. Diagnostic criteria for multiple sclerosis: 2010 revisions to the McDonald criteria. Ann Neurol 2011;69(2):292–302.

21. Jovicich J, Czanner S, Greve D, et al. Reliability in multi-site structural MRI studies: effects of gradient non-linearity correction on phantom and human data. Neuroimage 2006;30(2):436–443.

22. Bodammer N, Kaufmann J, Kanowski M, Tempelmann C. Eddy current correction in diffusion-weighted imaging using pairs of images acquired with opposite diffusion gradient polarity. Magn Reson Med 2004;51(1):188–193.

23. Chiang CW, Wang Y, Sun P, et al. Quantifying white matter tract diffusion parameters in the presence of increased extra-fiber cellularity and vasogenic edema. Neuroimage 2014;101:310–319.

24. Wang Y, Sun P, Wang Q, et al. Differentiation and quantification of inflammation, demyelination and axon injury or loss in multiple sclerosis. Brain 2015;138(Pt 5):1223–1238.

25. Zhang H, Hubbard PL, Parker GJ, Alexander DC. Axon diameter mapping in the presence of orientation dispersion with diffusion MRI. Neuroimage 2011;56(3):1301–1315.